

## Properties of Airy-Gauss Beams in the Fractional Fourier Transform Plane

Yimin Zhou<sup>1, 2</sup>, Guoquan Zhou<sup>1, 2, \*</sup>, and Guoyun Ru<sup>3</sup>

**Abstract**—An analytical expression of an Airy-Gauss beam passing through a fractional Fourier transform (FRFT) system is derived. The normalized intensity distribution, phase distribution, centre of gravity, effective beam size, linear momentum, and kurtosis parameter of the Airy-Gauss beam are demonstrated in FRFT plane, respectively. The influence of the fractional order  $p$  on the normalized intensity distribution, phase distribution, centre of gravity, effective beam size, linear momentum, and kurtosis parameter of the Airy-Gauss beam are examined in FRFT plane. The fractional order  $p$  controls the normalized intensity distribution, phase distribution, centre of gravity, effective beam size, the linear momentum, and kurtosis parameter. The period of the normalized intensity, phase, and centre of gravity versus the fractional order  $p$  is 4. The period of effective beam size, linear momentum, and kurtosis parameter versus the fractional order  $p$  is 2. The periodic behaviors of the normalized intensity distribution, phase distribution, centre of gravity, effective beam size, linear momentum, and kurtosis parameter can bring novel applications such as optical switch, optical micromanipulation, and optical image processing.

### 1. INTRODUCTION

An Airy beam carries infinite energy and exhibits a non-spreading property in vacuum [1]. The Wigner distribution function [2] and wave analysis [3] have been used to explain the intriguing features of an Airy beam. The self-healing [4], Poynting vector and angular momentum [5], ballistic dynamics [6], beam propagation factor [7], fractional Fourier transform (FRFT) [8], and far-field divergent properties [9] of an Airy beam have been investigated, respectively. A finite-energy Airy beam can freely accelerate upon propagation [10, 11]. The propagation of an Airy beam in water [12], in a Kerr medium [13], in turbulence [14], and in photorefractive media [15], in a uniaxial crystal [16], in strongly nonlocal nonlinear media [17], and through an apertured and misaligned optical system [18] has been analyzed, respectively. By using the coherently combinative technology, a high-power Airy beam can be generated [19]. The Airy beam can be used in particle clearing [20], optical switching [21], optical trapping [22], and spatiotemporal measurement [23]. Due to carrying finite power, the Airy-Gauss beam is described in a more realistic way that the Airy beam propagates [24]. The propagation of the Airy-Gauss beam in strongly nonlocal nonlinear media has been examined [25]. The analytical vectorial structure of the Airy-Gauss beam has been presented in the far-field regime [26].

Suppose that a piece of graded-index fiber with a proper length  $L$  is available to perform a Fourier transform of an input image. If this graded-index fiber is cut into pieces, a piece of length  $pL$  ( $p$  is the order of FRFT) just performs the fractional Fourier transform of the input image. As an image can be uniquely described by a Wigner distribution function, the FRFT also indicates that the Wigner distribution function is rotated by an angle of  $\varphi = p\pi/2$  [27]. The FRFT has been widely used in the

---

Received 1 December 2014, Accepted 30 December 2014, Scheduled 4 January 2015

\* Corresponding author: Guoquan Zhou (zhouguoquan178@sohu.com).

<sup>1</sup> School of Sciences, Zhejiang A & F University, Lin'an 311300, P. R. China. <sup>2</sup> Zhejiang Provincial Key Laboratory of Chemical Utilization of Forestry Biomass, Zhejiang A & F University, Lin'an 311300, P. R. China. <sup>3</sup> ASML Inc., 77 Danbury Road, Wilton, CT 06897, USA.

beam analysis, beam shaping and signal processing [28]. The FRFTs of many kinds of laser beams have been investigated extensively [29–31]. However, the propagation of Airy-Gauss beam has not been studied by FRFT method so far. Moreover, the research in the FRFT of Airy-Gauss beams is beneficial to optical micromanipulation and can extend the application field of Airy-Gauss beams. In the remainder of this paper, therefore, the FRFT is applied to treating the propagation of Airy-Gauss beams. An analytical expression for the FRFT of an Airy-Gauss beam is derived, and the properties of the Airy-Gauss beam in the FRFT plane are illustrated in detail.

## 2. AIRY-GAUSS BEAMS PASSING THROUGH A FRACTIONAL FOURIER TRANSFORM SYSTEM

In the Cartesian coordinate system, the  $z$ -axis is taken to be the propagation axis. The initial distribution of an Airy-Gauss beam in the source plane  $z = 0$  is described by [25, 26]

$$E(x_0, y_0, 0) = Ai\left(\frac{x_0}{w_0}\right) Ai\left(\frac{y_0}{w_0}\right) \exp\left(-\frac{a\rho_0^2}{w_0^2}\right), \quad (1)$$

where  $\rho_0 = (x_0^2 + y_0^2)^{1/2}$ .  $w_0$  is the transverse scale,  $Ai(\cdot)$  the Airy function, and  $a$  the modulation parameter. First, let us investigate the beam propagation factor of the Airy-Gauss beam. As the beam propagation factor is an invariant, we calculate it in the source plane. According to the standard definition, the first-order moment of the Airy-Gauss beam in the  $j$ -direction is found to

$$\langle j_0 \rangle = \frac{\int_{-\infty}^{\infty} \int_{-\infty}^{\infty} j_0 |E(x_0, y_0, 0)|^2 dx_0 dy_0}{\int_{-\infty}^{\infty} \int_{-\infty}^{\infty} |E(x_0, y_0, 0)|^2 dx_0 dy_0} = w_0 \frac{\int_{-\infty}^{\infty} \tau Ai^2(\tau) \exp(-2a\tau^2) d\tau}{\int_{-\infty}^{\infty} Ai^2(\tau) \exp(-2a\tau^2) d\tau}, \quad (2)$$

where  $j_0 = x_0$  or  $y_0$ , and  $j = x$  or  $y$ . As the analytical expression of Eq. (2) is complicated, it is not listed here. The second-order moment of the Airy-Gauss beam in the  $j$ -direction of the spatial domain reads as

$$\langle j_0^2 \rangle = \frac{\int_{-\infty}^{\infty} \int_{-\infty}^{\infty} (j_0 - \langle j_0 \rangle)^2 |E(x_0, y_0, 0)|^2 dx_0 dy_0}{\int_{-\infty}^{\infty} \int_{-\infty}^{\infty} |E(x_0, y_0, 0)|^2 dx_0 dy_0} = w_0^2 \frac{\int_{-\infty}^{\infty} \tau^2 Ai^2(\tau) \exp(-2a\tau^2) d\tau}{\int_{-\infty}^{\infty} Ai^2(\tau) \exp(-2a\tau^2) d\tau} - \langle j_0 \rangle^2, \quad (3)$$

The second-order moments of the Airy-Gauss beam in the  $j$ -direction of the frequency domain yield

$$\langle \theta_j^2 \rangle = \frac{\int_{-\infty}^{\infty} \int_{-\infty}^{\infty} \left| \frac{\partial E(x_0, y_0, 0)}{\partial j_0} \right|^2 dx_0 dy_0}{k^2 \int_{-\infty}^{\infty} \int_{-\infty}^{\infty} |E(x_0, y_0, 0)|^2 dx_0 dy_0} = \frac{1}{k^2 w_0^2} \frac{\int_{-\infty}^{\infty} [Ai'(\tau) - 2a\tau Ai(\tau)]^2 \exp(-2a\tau^2) d\tau}{\int_{-\infty}^{\infty} Ai^2(\tau) \exp(-2a\tau^2) d\tau}, \quad (4)$$

where  $k = 2\pi/\lambda$  is the wave number with  $\lambda$  being the optical wavelength, and  $Ai'(\cdot)$  is the Airyprime function. The cross second-order moment in the  $j$ -direction of the source plane is given by

$$\langle j_0 \theta_j \rangle = \frac{\pi}{ik} \frac{\int_{-\infty}^{\infty} \int_{-\infty}^{\infty} \left\{ j_0 \left[ \frac{\partial E(x_0, y_0, 0)}{\partial j_0} \right]^* E(x_0, y_0, 0) - j_0 \frac{\partial E(x_0, y_0, 0)}{\partial j_0} [E(x_0, y_0, 0)]^* \right\} dx_0 dy_0}{\int_{-\infty}^{\infty} \int_{-\infty}^{\infty} |E(x_0, y_0, 0)|^2 dx_0 dy_0} = 0, \quad (5)$$

where the asterisk denotes the complex conjugation. The  $M_j^2$  factor of the Airy-Gauss beam is given by

$$M_j^2 = 2k \left( \langle j_0^2 \rangle \langle \theta_j^2 \rangle - \langle j_0 \theta_j \rangle^2 \right)^{1/2} = 2k \sqrt{\langle j_0^2 \rangle \langle \theta_j^2 \rangle}. \quad (6)$$

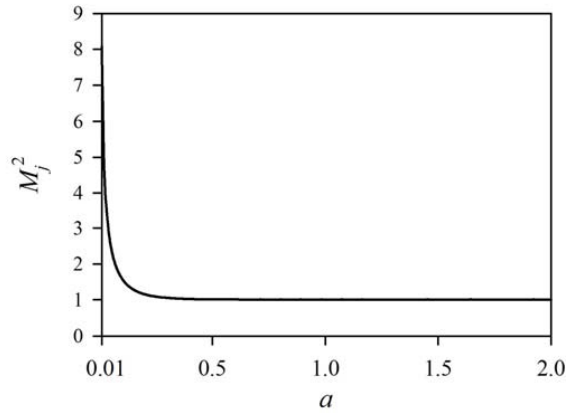


**Figure 1.** The beam propagation factor as a function of the modulation parameter  $a$ .

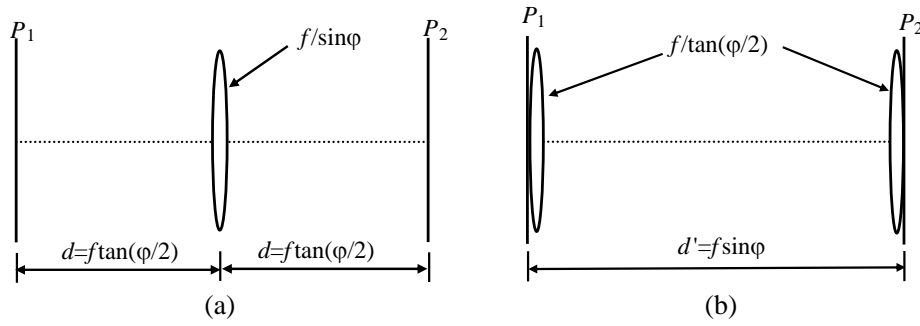


**Figure 2.** Optical system for performing the fractional Fourier transform. (a) Lohmann I system. (b) Lohmann II system.

The beam propagation factor of the Airy-Gauss beam only depends on the modulation parameter  $a$ . Fig. 1 represents the beam propagation factor as a function of the modulation parameter  $a$ . As the modulation parameter  $a$  tends to zero, the beam propagation factor tends to infinity. When the modulation parameter is equal to zero, the Airy-Gauss beam reduces to be a Airy beam and carries infinite energy. Therefore, the starting value of the modulation parameter  $a$  in Fig. 1 is 0.01. With increasing the modulation parameter  $a$ , the beam propagation factor quickly decreases and tends to the saturated value 1. When the modulation parameter  $a$  is relatively large, the Airy-Gauss beam is predominated by the Gaussian part. When the modulation parameter  $a$  is small, the Airy-Gauss beam is predominated by the Airy part.

Optical system for performing the fractional Fourier transform is shown in Fig. 2. Fig. 2(a) denotes the Lohmann I system, and Fig. 2(b) corresponds to the Lohmann II system.  $P_1$  and  $P_2$  are the input and output planes, respectively. The input plane is just the source plane of the Airy-Gauss beam.  $f$  is the standard focal length. The focus of the spherical lens is  $f/\sin\varphi$  in Fig. 2(a) and  $f/\tan(\varphi/2)$  in Fig. 2(b). The distance between the input and output planes is  $2d = 2f \tan(\varphi/2)$  in Fig. 2(a) and  $d' = f \sin\varphi$  in Fig. 2(b). The Lohmann I and II optical systems are equivalent and are described by the following transfer matrix

$$\begin{pmatrix} A & B \\ C & D \end{pmatrix} = \begin{pmatrix} \cos\varphi & f \sin\varphi \\ -\sin\varphi/f & \cos\varphi \end{pmatrix}. \tag{7}$$

The Airy-Gauss beam passing through a Lohmann optical system obeys the well-known Collins integral formula:

$$E(x, y) = \frac{\exp(ikz)}{i\lambda B} \int_{-\infty}^{\infty} \int_{-\infty}^{\infty} E(x_0, y_0, 0) \exp \left\{ \frac{ik}{2B} [A\rho_0^2 - 2(x_0x + yy_0) + D\rho^2] \right\} dx_0 dy_0, \tag{8}$$

where  $\rho = (x^2 + y^2)^{1/2}$ . Inserting Eq. (1) into Eq. (8), we can obtain

$$E(x, y) = \frac{1}{i\lambda B} \exp\left(ikz + \frac{ikD}{2B}\rho^2\right) U(x)U(y) \quad (9)$$

with  $U(x)$  and  $U(y)$  given by

$$U(j) = \exp\left(-\frac{k^2 j^2}{4\beta B^2}\right) \left[ f_1\left(-\frac{ikj}{2\beta B}\right) \otimes f_2\left(-\frac{ikj}{2\beta B}\right) \right], \quad (10)$$

where  $\beta = \frac{a}{w_0^2} - \frac{ikA}{2B}$ ,  $f_1(\tau) = Ai\left(\frac{\tau}{w_0}\right)$ , and  $f_2(\tau) = \exp(-\beta\tau^2)$ . “ $\otimes$ ” denotes the convolution. The convolution theorem of the Fourier transformation has the following property [32]

$$f_1(\tau) \otimes f_2(\tau) = \int_{-\infty}^{\infty} f_1(\xi)f_2(\xi) \exp(-i\xi\tau)d\xi, \quad (11)$$

where the auxiliary functions  $f_1(\xi)$  and  $f_2(\xi)$  are the Fourier transformation of  $f_1(\tau)$  and  $f_2(\tau)$ , respectively.  $f_1(\xi)$  and  $f_2(\xi)$  are given by [32]

$$f_1(\xi) = \frac{1}{\sqrt{2\pi}} \int_{-\infty}^{\infty} Ai\left(\frac{\tau}{w_0}\right) \exp(i\xi\tau)d\tau = \frac{w_0}{\sqrt{2\pi}} \exp\left(-\frac{iw_0^3}{3}\xi^3\right), \quad (12)$$

$$f_2(\xi) = \frac{1}{\sqrt{2\pi}} \int_{-\infty}^{\infty} \exp(-\beta\tau^2) \exp(i\xi\tau)d\tau = \sqrt{\frac{1}{2\beta}} \exp\left(-\frac{\xi^2}{4\beta}\right). \quad (13)$$

After performing the complicated integral, Eq. (10) can be analytically expressed as

$$U(j) = \sqrt{\frac{\pi}{\beta}} Ai\left(\frac{-ikj}{2w_0\beta B} + \frac{1}{16\beta^2 w_0^4}\right) \exp\left(-\frac{k^2 j^2}{4\beta B^2} - \frac{ikj}{8B\beta^2 w_0^3} + \frac{1}{96\beta^3 w_0^6}\right). \quad (14)$$

Accordingly, the Airy-Gauss beam in FRFT plane reads as

$$\begin{aligned} E(x, y) &= \frac{\pi}{i\lambda\beta B} \exp\left(ikz + \frac{ikD}{2B}\rho^2\right) Ai\left(\frac{-ikx}{2w_0\beta B} + \frac{1}{16\beta^2 w_0^4}\right) Ai\left(\frac{-iky}{2w_0\beta B} + \frac{1}{16\beta^2 w_0^4}\right) \\ &\times \exp\left[-\frac{k^2\rho^2}{4\beta B^2} - \frac{ik(x+y)}{8B\beta^2 w_0^3} + \frac{1}{48\beta^3 w_0^6}\right]. \end{aligned} \quad (15)$$

The centre of gravity of the Airy-Gauss beam in the  $j$ -direction of the FRFT plane is given by

$$j_C = \frac{\int_{-\infty}^{\infty} \int_{-\infty}^{\infty} j |E(x, y)|^2 dx dy}{\int_{-\infty}^{\infty} \int_{-\infty}^{\infty} |E(x, y)|^2 dx dy} = \frac{\int_{-\infty}^{\infty} j |U(j)|^2 dj}{\int_{-\infty}^{\infty} |U(j)|^2 dj}. \quad (16)$$

The effective beam size of the Airy-Gauss beam in the  $j$ -direction of the FRFT plane turns out to be [33]:

$$W_j = [2\langle(j - j_C)^2\rangle]^{1/2} = \left[2\frac{\int_{-\infty}^{\infty} (j - j_C)^2 |U(j)|^2 dj}{\int_{-\infty}^{\infty} |U(j)|^2 dj}\right]^{1/2}. \quad (17)$$

The linear momentum of the Airy-Gauss beam in the  $j$ -direction of the FRFT plane is found to be [34]

$$Q_j = -\frac{i}{2} \int_{-\infty}^{\infty} \int_{-\infty}^{\infty} \left[ E^*(x, y) \frac{\partial E(x, y)}{\partial j} - E(x, y) \frac{\partial E^*(x, y)}{\partial j} \right] dx dy. \quad (18)$$

The kurtosis parameter, which is employed to describe the flatness degree of the beams, is an important parameter to evaluate the beam propagation. The kurtosis parameter in the  $j$ -direction of the FRFT plane yields [35]

$$K_j = \frac{\langle(j - j_C)^4\rangle}{\langle(j - j_C)^2\rangle^2} = \frac{4\langle(j - j_C)^4\rangle}{W_j^4}. \quad (19)$$

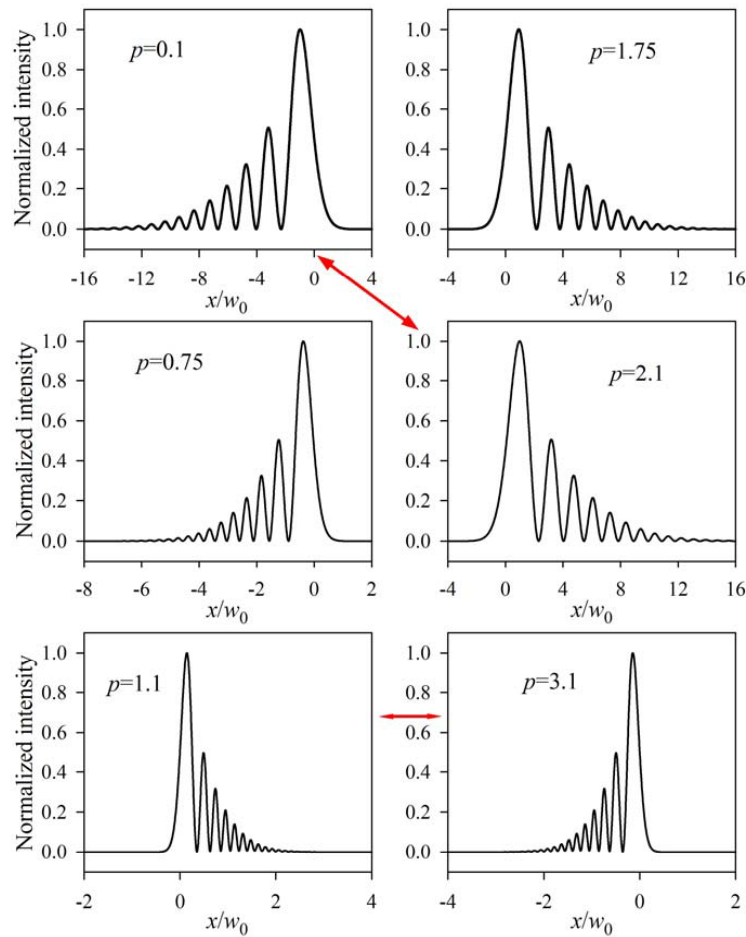


**Figure 3.** Normalized intensity distribution in the  $x$ -direction of an Airy-Gauss beam with different fractional order  $p$  in the FRFT plane.

### 3. NUMERICAL CALCULATIONS AND ANALYSES

Based on the formulae derived in the section above, the properties of an Airy-Gauss beam in the FRFT plane are numerically investigated. The  $x$ - and  $y$ -directions are separable in the formulae derived above. Moreover, they have the same form. Therefore, hereafter we only consider the  $x$ -direction. Here we mainly pay attention to the influence of the fractional order  $p$  on the propagation of an Airy-Gauss beam. Calculation parameters are chosen as  $\lambda = 0.53 \mu\text{m}$ ,  $w_0 = 1 \text{ mm}$ ,  $a = 0.01$ , and  $f = 1000 \text{ mm}$ , which is one of the general cases. Fig. 3 represents the contour graph of the normalized intensity distribution in the  $x$ -direction of an Airy-Gauss beam with different fractional order  $p$  in the FRFT plane. The selection of the values for  $p$  is to show the evolution law of the normalized intensity distribution versus the fractional order  $p$ . The normalized intensity distribution versus the fractional order  $p$  is periodic, and the period is 4. When  $0 < p < 1$  and  $3 < p < 4$ , the lateral side lobes are located at the left side. When  $1 < p < 3$ , the lateral side lobes are located at the right side. When the difference of the two fractional orders is half period 2, the two normalized intensity distributions are reversal mutually, which is shown as  $p = 0.1$  and  $p = 2.1$  or  $p = 1.1$  and  $p = 3.1$ . The phase distribution in the  $x$ -direction of an Airy-Gauss beam with different fractional order  $p$  in the FRFT plane is shown in Fig. 4. The period of the phase versus the fractional order  $p$  is also 4. The fluctuation of the phase where the dominant lobe is located is the smallest, which is marked with a circle in red. The reversal phenomenon that appears in the normalized intensity distribution also happens to the phase distribution.

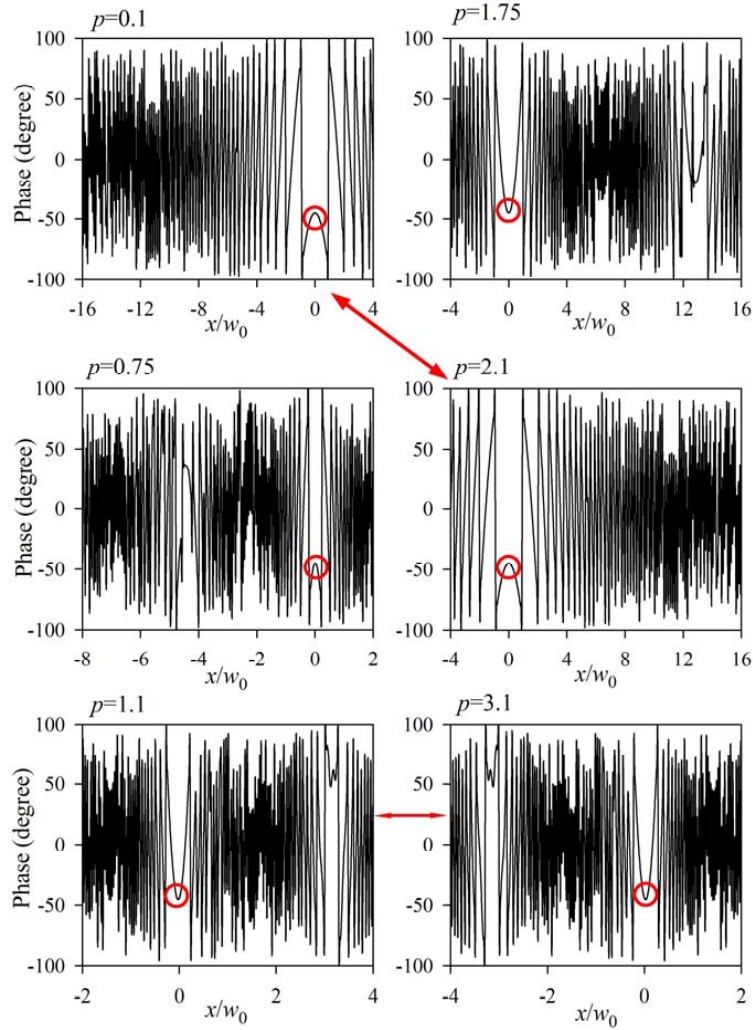


**Figure 4.** The phase distribution in the  $x$ -direction of an Airy-Gauss beam with different fractional order  $p$  in the FRFT plane.

The centre of gravity, effective beam size, linear momentum, and kurtosis parameter in the  $x$ -direction as a function of the fractional order  $p$  are shown in Fig. 5. The period of the centre of gravity versus fractional order  $p$  is 4. In the first half period, the centre of gravity increases from the minimum value to the maximum one with increasing the value of the fractional order  $p$ . In the last half period, the centre of gravity decreases from the maximum value to the minimum one with increasing the value of fractional order  $p$ . The period of the effective beam size versus the fractional order  $p$  is 2. In the first half period, the effective beam size decreases from the maximum value to the minimum one with increasing the value of fractional order  $p$ . In the last half period, the effective beam size increases from the minimum value to the maximum one with increasing the value of the fractional order  $p$ . The period of the linear momentum versus the fractional order  $p$  is 2. The minus sign only denotes the direction of the linear momentum. In the first half period, the linear momentum increases from zero to the maximum value with increasing the value of fractional order  $p$ . In the last half period, the linear momentum decreases from the maximum value to zero with increasing the value of fractional order  $p$ . The period of the kurtosis parameter versus fractional order  $p$  is also 2. In the first half period, the kurtosis parameter increases from the minimum value to the maximum one with increasing the value of fractional order  $p$ . In the last half period, the kurtosis parameter decreases from the maximum value to the minimum one with increasing the value of fractional order  $p$ . The kurtosis parameter represents

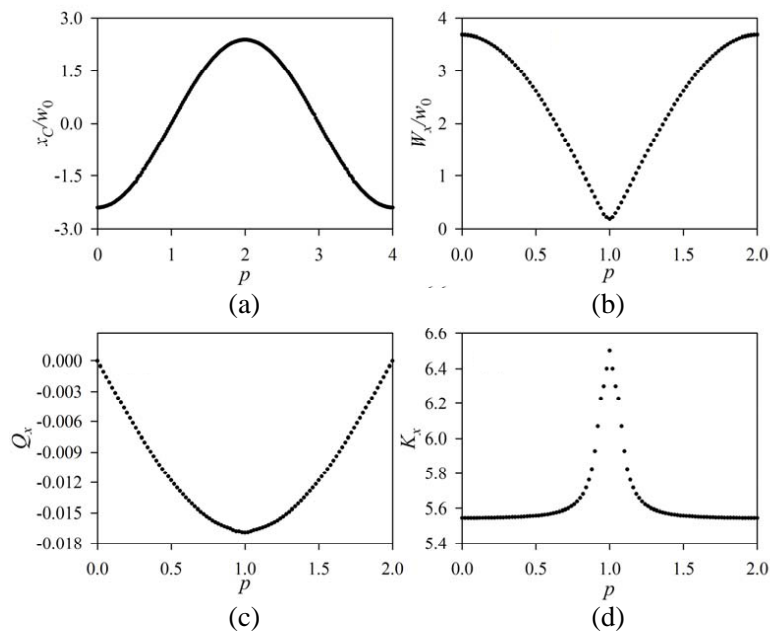


**Figure 5.** (a) The centre of gravity, (b) the effective beam size, (c) the linear momentum, and (d) the kurtosis parameter in the  $x$ -direction as a function of the fractional order  $p$ .

the degree of sharpness of the beam intensity distribution. In the case of  $p = 1$ , the effective beam size reaches the minimum value, and the corresponding kurtosis parameter has the largest value. When  $p$  is far away from 1, the kurtosis parameter has nearly the same value.

#### 4. CONCLUSIONS

The period of the normalized intensity, phase, and centre of gravity versus fractional order  $p$  is 4. The period of the effective beam size, linear momentum, and kurtosis parameter versus fractional order  $p$  is 2. In the first and last quarters of the period, the lateral side lobes are located at the left side. Otherwise, the lateral side lobes are located at the right side. With increasing the value of fractional order  $p$  in the first half period, the centre of gravity, linear momentum, and kurtosis parameter increase, while the effective beam size decreases. With increasing the value of the fractional order  $p$  in the last half period, the centre of gravity, linear momentum, and kurtosis parameter decrease; however, the effective beam size increases. When the difference of the two fractional orders is the half period, the two normalized intensity distributions or the two phase distributions are mutual reversal. This research could bring novel applications. The reversal phenomenon in the intensity and phase distributions can be used as optical switch. The behavior of linear momentum can be used in optical micromanipulation. This research is also useful to the optical image processing involving the fractional Fourier transform [36, 37]. In [36], the order of FRFT effectively enhances the security of image processing system. In the decryption process, the phase-only mask with false information and the other two phase-only masks are respectively placed in the input and fractional Fourier planes to recover the primary image. An imaging algorithm with application of FRFT for ground moving train imaging by Ku-band ground-based radar has been introduced in [37], and the multiple Doppler parameters are estimated from different sections of data in FRFT domain.

#### ACKNOWLEDGMENT

This research was supported by the National Natural Science Foundation of China under Grant Nos. 61178016 and 51103136, and Zhejiang Provincial Natural Science Foundation of China under Grant No. Y1090073. The authors are indebted to the reviewers for their valuable comments.

## REFERENCES

1. Berry, M. V. and N. L. Balazs, "Nonspreading wave packets," *Am. J. Phys.*, Vol. 47, 264–267, 1979.
2. Chen, R. P., H. P. Zheng, and C. Q. Dai, "Wigner distribution function of an Airy beam," *J. Opt. Soc. Am. A*, Vol. 28, 1307–1311, 2011.
3. Kaganovsky, Y. and E. Heyman, "Wave analysis of Airy beams," *Opt. Express*, Vol. 18, 8440–8452, 2010.
4. Brokly, J., G. A. Siviloglou, A. Dogariu, and D. N. Christodoulides, "Self-healing properties of optical Airy beams," *Opt. Express*, Vol. 16, 12880–12891, 2008.
5. Sztul, H. I. and R. R. Alfano, "The Poynting vector and angular momentum of Airy beams," *Opt. Express*, Vol. 16, 9411–9416, 2008.
6. Siviloglou, G. A., J. Brokly, A. Dogariu, and D. N. Christodoulides, "Ballistic dynamics of Airy beams," *Opt. Lett.*, Vol. 33, 207–209, 2008.
7. Chen, R. P. and C. F. Ying, "Beam propagation factor of an Airy beam," *J. Opt.*, Vol. 13, 085704, 2011.
8. Zhou, G. Q., R. P. Chen, and X. X. Chu, "Fractional Fourier transform of Airy beams," *Appl. Phys. B*, Vol. 109, 549–556, 2012.
9. Xu, Y. Q. and G. Q. Zhou, "The far-field divergent properties of an Airy beam," *Opt. & Laser Tech.*, Vol. 44, 1318–1323, 2012.
10. Siviloglou, G. A., J. Brokly, A. Dogariu, and D. N. Christodoulides, "Observation of accelerating Airy beam," *Phys. Rev. Lett.*, Vol. 99, 213901, 2007.
11. Siviloglou, G. A. and D. N. Christodoulides, "Accelerating finite energy Airy beams," *Opt. Lett.*, Vol. 32, 979–981, 2007.
12. Polynkin, P., M. Kolesik, and J. Moloney, "Filamentation of femtosecond laser Airy beams in water," *Phys. Rev. Lett.*, Vol. 103, 123902, 2009.
13. Chen, R. P., C. F. Yin, X. X. Chu, and H. Wang, "Effect of Kerr nonlinearity on an Airy beam," *Phys. Rev. A*, Vol. 82, 043832, 2010.
14. Chu, X. X., "Evolution of an Airy beam in turbulence," *Opt. Lett.*, Vol. 36, 2701–2703, 2011.
15. Jia, S., J. Lee, J. W. Fleischer, G. A. Siviloglou, and D. N. Christodoulides, "Diffusion-trapped Airy beams in photorefractive media," *Phys. Rev. Lett.*, Vol. 104, 253904, 2010.
16. Zhou, G. Q., R. P. Chen, and X. X. Chu, "Propagation of Airy beams in uniaxial crystals orthogonal to the optical axis," *Opt. Express*, Vol. 20, 2196–2205, 2012.
17. Zhou, G. Q., R. P. Chen, and G. Y. Ru, "Propagation of an Airy beam in a strongly nonlocal nonlinear media," *Laser Phys. Lett.*, Vol. 11, 105001, 2014.
18. Wen, W., X. Y. Lu, C. L. Zhao, and Y. J. Cai, "Propagation of Airy beam passing through the misaligned optical system with hard aperture," *Opt. Commun.*, Vol. 313, 350–355, 2014.
19. Chu, X. X., Z. J. Liu, and P. Zhou, "Generation of a high-power Airy beam by coherent combining technology," *Laser Phys. Lett.*, Vol. 10, 125102, 2013.
20. Baumgartl, J., M. Mazilu, and K. Dholakia, "Optically mediated particle clearing using Airy wavepackets," *Nature Photon.*, Vol. 2, 675–678, 2008.
21. Ellenbogen, T., N. Voloch-Bloch, A. Ganany-Padowicz, and A. Arie, "Nonlinear generation and manipulation of Airy beams," *Nature Photon.*, Vol. 3, 395–398, 2009.
22. Lu, W., J. Chen, Z. Lin, and S. Liu, "Driving a dielectric cylindrical particle with a one dimensional airy beam: A rigorous full wave solution," *Progress In Electromagnetics Research*, Vol. 115, 409–422, 2011.
23. Piksarv, P., A. Valdmann, H. Valtna-Lukner, and P. Saari, "Ultrabroadband Airy light bullets," *Laser. Phys.*, Vol. 24, 085301, 2014.
24. Bandres, M. A. and J. C. Gutiérrez-Vega, "Airy-Gauss beams and their transformation by paraxial optical systems," *Opt. Express*, Vol. 15, 16719–16728, 2007.
25. Deng, D. M. and H. Li, "Propagation properties of Airy-Gaussian beam," *Appl. Phys. B*, Vol. 106, 677–681, 2012.

26. Deng, X. B., D. M. Deng, C. Chen, and C. Y. Liu, "Analytical vectorial structure of Airy-Gaussian beam," *Acta Phys. Sin.*, Vol. 62, 174201, 2013.
27. Lohmann, A. W., "Image rotation, Wigner rotation, and the fractional Fourier transform," *J. Opt. Soc. Am. A*, Vol. 10, 2181–2186, 1993.
28. Namias, V., "The fractional order Fourier transform and its application to quantum mechanics," *J. Inst. Math. Appl.*, Vol. 25, 241–265, 1980.
29. Cai, Y. J. and Q. Lin, "Transformation and spectrum properties of partially coherent beams in the fractional Fourier transform plane," *J. Opt. Soc. Am. A*, Vol. 20, 1528–1536, 2003.
30. Du, X. Y. and D. M. Zhao, "Fractional Fourier transform of truncated elliptical Gaussian beams," *Appl. Opt.*, Vol. 45, 9049–9052, 2006.
31. Zhou, G. Q., "Fractional Fourier transform of Lorentz-Gauss beams," *J. Opt. Soc. Am. A*, Vol. 26, 350–355, 2009.
32. Gradshteyn, I. S. and I. M. Ryzhik, *Table of Integrals, Series, and Products*, Academic Press, New York, 1980.
33. Carter, W. H., "Spot size and divergence for Hermite Gaussian beams of any order," *Appl. Opt.*, Vol. 19, 1027–1029, 1980.
34. Yakimenko, A. I., V. M. Lashkin, and O. O. Prikhodko, "Dynamics of two-dimensional coherent structures in nonlocal nonlinear media," *Phys. Rev. E*, Vol. 73, 066605, 2006.
35. Bock, B. D., *Multivariate Statistical Method in Behavioral Research*, McGraw-Hill, New York, 1975.
36. Dai, C. Q., X. G. Wang, G. Q. Zhou, and J. L. Chen, "Optical image-hiding method with false information disclosure based on the interference principle and partial-phase-truncation in the fractional Fourier domain," *Laser Phys. Lett.*, Vol. 11, 075603, 2014.
37. Yu, L. and Y. Zhang, "Application of the fractional fourier transform to moving train imaging," *Progress In Electromagnetics Research M*, Vol. 19, 13–23, 2011.